Large-amplitude easy-plane spin-orbit torque oscillators driven by out-of-plane spin current: A micromagnetic study

Daniel Kubler,[1] David A. Smith,[2,3] Tommy Nguyen,[1] Fernando Ramos-Diaz,[2] Satoru Emori,[2,4,*] and Vivek P. Amin[1,†]

[1] *Department of Physics, Indiana University, Indianapolis, IN 46202, USA*
[2] *Department of Physics, Virginia Tech, Blacksburg, VA 24061, USA*
[3] *HRL Laboratories, Malibu, CA 90265*
[4] *Academy of Integrated Science, Virginia Tech, Blacksburg, VA 24061, USA*

(Dated: December 18, 2024)

Spin torque oscillators generate a periodic output signal from a non-periodic input, making them promising candidates for applications like microwave communications and neuromorphic computing. However, traditional spin torque oscillators suffer from a limited precessional cone angle and thermal stability, as well as a need for an applied bias magnetic field. We use micromagnetic simulations to demonstrate a novel spin torque oscillator that relies on spin-orbit effects in ferromagnets to overcome these limitations. The key mechanism behind this oscillator is the generation of an *out-of-plane spin current*, in which both the spin flow and the spin orientation are out-of-plane. The torque from this spin current enables easy-plane coherent magnetic precession with a large cone angle and high thermal stability over a micron-scale lateral area. Moreover, the precession occurs about an internal field in the free layer, thereby eliminating the need for an external bias field. We find that the ratio of the unconventional out-of-plane spin current to the conventional spin-Hall spin current can be as low as 4% and still result in bias-field-free, room temperature, self-sustained oscillations. Our results are fundamentally important in demonstrating that a small ratio of unconventional to conventional spin currents critically affects magnetization dynamics. Our findings also provide a theoretical proof-of-concept of a novel spintronic device with promising applications.

I. INTRODUCTION

Devices that efficiently convert a dc input into a self-sustaining ac signal are crucial to a wide variety of fields from microwave communications to neuromorphic computing [1–3]. Spin torque oscillators are promising building blocks for such applications due to their GHz oscillation frequencies and purported energy efficiency [4–7]. In any spin-torque oscillator, the magnetic order parameter of the magnetic free layer self-oscillates under a dc electrical current input. In particular, the self-sustained oscillations are driven by a spin torque, i.e., a transfer of spin angular momentum from an incident spin-polarized current to the magnetization of a ferromagnetic layer [8, 9]. The spin torque effectively cancels magnetic damping in the free layer – thereby allowing the magnetization to precess freely about a magnetic field. The precessing magnetization generates an oscillating electrical voltage output, i.e., the product of the dc current and the time-varying magnetoresistance. For high power output from a spin torque oscillator, it is critical to stabilize a large cone angle for magnetic precession.

To date, there are two major types of spin-torque oscillators. The first is spin-transfer torque oscillators, illustrated in Fig. 1(a), that are based on current-out-of-plane nanoscale devices. In this device scheme, a charge current is passed along the vertical axis, which includes a magnetic "fixed layer." The current becomes spin-polarized by the fixed layer and then imparts a spin-transfer torque on the free layer magnetization. Spin-transfer torque oscillators were originally based on all-metal structures, such as mechanical point-contacts [10, 11], nanopillars of spin valves [7, 12], and nanocontacts on top of spin valves [13]. Later, nanopillars and nanocontacts based on magnetic tunnel junctions [14–16] were developed to leverage the large tunnel magnetoresistance response. Yet, a major drawback is that the electric current must pass through a resistive tunnel barrier, which leads to high power dissipation and durability issues from dielectric breakdown [17]. For all current-out-of-plane spin-transfer torque oscillators, another practical disadvantage is that the effective free-layer area must be $\lesssim 0.01\,\mu m^2$ to prevent magnetization curling (e.g., from the current-induced Oersted field) and to achieve uniform dynamics for GHz-range output [18, 19]. The small active area makes the oscillations vulnerable to thermal fluctuations [20], reducing the oscillator's signal output and quality factor.

The second type is the spin-orbit torque oscillator, illustrated in Fig. 1(b), which possesses a simpler planar device structure that overcomes some of the disadvantages of the spin-transfer torque oscillator. A typical spin-orbit torque oscillator consists of a magnetic free layer interfaced with a metal with a strong spin-orbit effect (e.g., spin-Hall effect), such as Pt [21, 22]. An in-plane charge current generates a spin current, which flows out-of-plane and exerts a "spin-orbit torque" on the magnetization in the adjacent free layer [23]. The

* semori@vt.edu
† vpamin@iu.edu

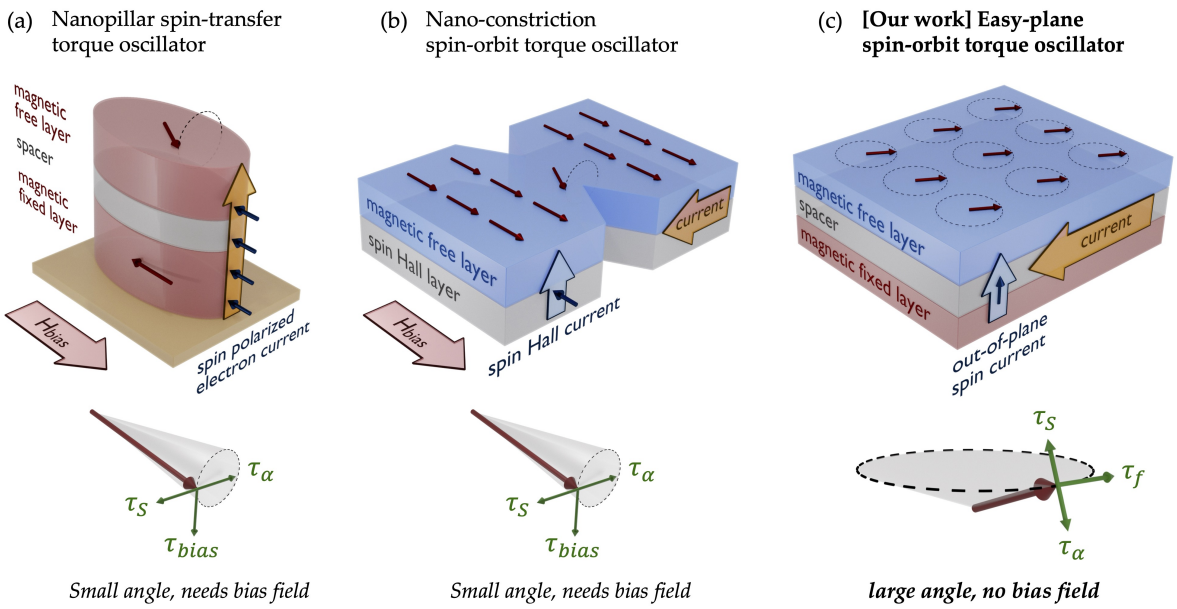

FIG. 1. (a) Conventional spin-transfer torque oscillator with out-of-plane charge current and bias magnetic field $H_{\rm bias}$. Dark red arrows represent magnetization and blue arrows represent the magnetic moment of carriers (oriented antiparallel to the spin). The magnetic fixed layer spin-polarizes the electrical current which is absorbed by the magnetic free layer, imparting a spin-transfer torque $\tau_{\rm S}$. The role of the spin transfer torque is to cancel the damping torque τ_α, enabling the free layer magnetization to precess about the bias magnetic field (with corresponding torque $\tau_{\rm bias}$). (b) Conventional spin-orbit torque oscillator with in-plane charge current and bias magnetic field. The bottom layer, typically a heavy metal, converts an in-plane charge current into a spin current flowing out-of-plane. Like (a), the spin current is then absorbed by the magnetic free layer, imparts a spin torque $\tau_{\rm S}$ that compensates the damping τ_α, and enables magnetization precession about the bias magnetic field (with corresponding torque $\tau_{\rm bias}$). Both (a) and (b) suffer from small output signal, thermal instability, and the requirement of a bias field for operation. (c) Our proposed device, an easy-plane spin-orbit torque oscillator, with in-plane charge current and no bias magnetic field. The in-plane charge current in the magnetic fixed layer generates an out-of-plane spin current that flows to the magnetic free layer and imparts a spin torque $\tau_{\rm S}$. The spin torque tilts the magnetic moments out-of-plane and compensates the material's damping τ_α, enabling oscillations around an internal field, e.g., demagnetization field (with corresponding torque $\tau_{\rm f}$). The torque diagram below each device shows the torques necessary for each to undergo self-sustained oscillations and highlights the large precessional cone angle for the newly proposed device (c).

driving charge current does not need to pass through a resistive tunnel barrier, thereby permitting lower power consumption and higher device durability [18, 24]. Further, the spin-orbit torque oscillator requires a minimum of just two steps of lithography and is easier to fabricate than nanopillars. Therefore, substantial effort has been devoted recently to the development of spin-orbit torque oscillators for microwave electronics and neuromorphic computing [25–29].

However, existing spin-orbit torque oscillators exhibit serious drawbacks. First, they have small precessional cone angles of $<20°$ [30] and rely on small anisotropic magnetoresistance ratio of $<1\%$ [18, 31]. Hence, a single spin-orbit torque oscillator typically has a small power output. The spin-orbit torque from a spin-Hall current also cannot sustain coherent oscillations over a large lateral area in an individual device, due to scattering of the coherent mode into different magnon modes [32–35]. Uniform, coherent oscillations can be stabilized only within a small area of $<0.1\,\mu{\rm m}^2$, requiring deep-submicron lithography for nanoscale confinement [32, 36] – e.g., the nano-constriction geometry illustrated in Fig. 1(b). The small active area results in greater instability from thermal fluctuations [18], curtailing the quality-factor [24, 25, 36] or limiting self-oscillations to cryogenic temperatures [32]. It is possible to extend the active area, and therefore stability, by mutually synchronizing a chain or array of spin-orbit torque oscillators fabricated with high-resolution nano-lithography [25, 26, 37]. Still, there remains a general issue with existing spin-orbit torque oscillators: they require a bias field to set the axis of precession. While the oscillators themselves could be compact, the need for a bias magnet would make the overall device architecture quite cumbersome.

In this paper, we present micromagnetic simulations on novel *large-amplitude, easy-plane* spin-orbit torque oscillators that overcome the difficulties plaguing the traditional spin-torque oscillators. The proposed device resembles a current-in-plane spin valve exhibiting giant magnetoresistance, illustrated in Fig. 1(c), consisting of a fixed magnetic layer and a free magnetic layer. An

in-plane direct current in the fixed layer drives coherent easy-plane oscillations in the free layer approaching 90° cone angle over a micron-scale lateral area.

The key to this new easy-plane oscillator is the spin-orbit effects in the fixed layer to generate an *out-of-plane spin current*, i.e. a spin current with out-of-plane flow and spin orientation. This out-of-plane spin current is guaranteed by symmetry [38–40] and quantified in theoretical work [40–46]. Unconventional (non-spin-Hall) spin currents have been reported to emerge from various types of lateral structural symmetry breaking [47–50] and are proposed to enhance the performance of spintronic memories [51]. More crucially, recent experiments report that spin-orbit effects in *commonly-used magnetic metals* produce unconventional spin currents [52–54], including sufficient out-of-plane spin currents to switch perpendicular magnetic free layers [55–57]. The latter is of particular interest because the fixed magnetic layer, already an inherent component of the spin valve [Fig. 1(c)], can serve as a convenient source of out-of-plane spin current. The spin current flows into the free layer and tilts the magnetic order slightly out-of-plane while opposing the intrinsic damping. The magnetic order precesses about a strong internal effective field rather than an external magnetic field [58], hence permitting precession with within the plane of the free layer [Fig. 1(c)]. This large-cone-angle precession, inspired by recent proposals of superfluid-like magnetization dynamics [58–64], is robust against magnon scattering and can remain coherent over a micron-scale lateral area. Thus, this novel spin-orbit torque oscillator is expected to attain (i) a large output signal through a large precession cone angle and giant magnetoresistance, (ii) high stability enabled by a large active area of coherent precession, and (iii) zero-bias-field operation with the precession axis defined by an internal effective field.

An important question is whether realistic spin-orbit effects in the fixed ferromagnetic layer can enable the proposed coherent easy-plane precession. Recent studies indicate that in typical ferromagnetic metals, the magnitude of the out-of-plane spin current may be ∼10% [43, 46] or more than 200% [65] of the "in-plane" spin-Hall current. Our micromagnetic simulations demonstrate that coherent easy-plane precession can indeed be realized even when the out-of-plane spin current is just <10% of the total spin current. Further, micron-scale coherence of the easy-plane precession is maintained even when thermal fluctuations (corresponding to room temperature) are included. These robust features make the easy-plane spin-orbit torque oscillator a good candidate for emerging spintronic applications.

II. DESCRIPTION OF DEVICE

A. Device geometry and material composition

Our proposed device has a lateral area on the order of $1\,\mu m^2$, much greater than the nanopillar and nanoconstriction oscillators. In this study, we focus on a free layer comprised of a synthetic antiferromagnet [66], i.e., *two* ferromagnetic layers coupled antiparallely via the Ruderman-Kittel-Kasuya-Yosida (RKKY) interaction [67]. A free layer consisting of one ferromagnetic film cannot stabilize coherent, self-sustained oscillations over a μm^2 scale area; dipolar fields from the edges tend to break up a uniform precession mode into multiple precession modes with various phases [58, 61], analogous to the breakup of a single domain magnetization into multiple domains in a large area. The synthetic antiferromagnet greatly reduces the edge dipolar fields via flux closure [68], hence permitting uniform, coherent large cone-angle precession over the large lateral area[1]. The ability of the synthetic antiferromagnet to stabilize large cone-angle precession was previously demonstrated in simulations of superfluid-like spin transport [58, 61].

The easy-plane dynamics harks back to some families of spin-transfer torque oscillators driven by a vertical electrical current (see Fig. 1(a)). For instance, the torque from a perpendicular- or tilted-magnetization fixed layer was demonstrated to drive large cone-angle precession in the free layer [4, 69]. Synthetic antiferromagnetic free layers were also explored in nanopillar spin-transfer torque oscillators [70, 71], with a large operating window stabilizing large cone-angle precession of the interlayer-coupled magnetizations (e.g., "out-of-plane precession" in Ref. [71]). Nevertheless, we emphasize the key distinction: the spin-transfer torque oscillator [Fig. 1(a)] is limited to a nanoscale active area, whereas the easy-plane spin-orbit torque oscillator driven by an in-plane electric current [Fig. 1(c)] permits a much larger, micron-scale active area leading to higher stability.

In a macrospin picture, there are three key torques on the magnetization $\mathbf{m}$ in each layer of the synthetic antiferromagnet [Fig. 1(c)]:

1. The spin torque $\tau_{\mathbf{S}} \propto \mathbf{m} \times (\mathbf{m} \times \mathbf{s})$, from the injected spins $\mathbf{s}$, pulls $\mathbf{m}$ towards $\mathbf{s}$. This torque is often called a "damping-like" or "anti-damping" torque as it can counteract the damping inherent in the magnetic material. Out-of-plane polarized spins $\mathbf{s}||\hat{\mathbf{z}}$ cants the magnetization out-of-plane[2], generating a nonzero $\mathbf{z}$-component of $\mathbf{m}$.

[1] A free layer of synthetic *ferri*magnet, consisting of two ferromagnetic layers with slightly different thicknesses or saturation magnetizations, would also be sufficient for flux-closing the edge dipole fields [68] and hence support coherent easy-plane magnetic precession.

[2] In our micromagnetic simulations, we assume that the spin

2. The field torque $\tau_{\mathbf{f}} \propto -\mathbf{m} \times \mathbf{B}_{\mathbf{eff}}$ causes $\mathbf{m}$ to precess about the net effective field $\mathbf{B}_{\mathbf{eff}}$. Here, with the magnetization canted out-of-plane, $\mathbf{B}_{\mathbf{eff}}$ consists of the out-of-plane demagnetization field. In the synthetic antiferromagnet, the canted magnetization (misaligned with the other layer's magnetization) experiences an interlayer antiferromagnetic exchange field, which also contributes to $\mathbf{B}_{\mathbf{eff}}$. The magnetization sweeps a precessional orbit within the film plane.

3. The Gilbert damping torque $\tau_\alpha \sim \mathbf{m} \times (\mathbf{m} \times \mathbf{B}_{\mathbf{eff}})$ pulls $\mathbf{m}$ toward the film plane. In other words, the spin torque $\tau_{\mathbf{S}}$ must compete with the damping torque τ_α to cant the magnetization out-of-plane.

The tilt angle can be increased by increasing the out-of-plane spin current, which is done by increasing the in-plane charge current that generates it. Once the intrinsic damping torque is compensated by the spin torque, the magnetization is free to precess about the internal effective field [58]. The out-of-plane spin current and the internal field are the key enablers for the proposed device, as they remove the requirement for a bias magnetic field. In this work, we perform full micromagnetic simulations over a finite-sized device with a micron-scale lateral area, including edge effects and the generation of magnetization textures.

B. Types of spin current injection

In the magnetic fixed layer where the magnetization is parallel to the applied in-plane electric field (charge current), there are two types of spin currents allowed by symmetry: the spin-Hall current and an out-of-plane spin current [Fig. 2]. The spin-Hall effect produces a spin current such that the spin flow direction, spin orientation direction, and electric field direction are mutually orthogonal [74], as illustrated in Fig. 2(a). Both theoretical [75–77] and experimental [78–81] studies indicate that the spin-Hall conductivities σ_{SH} of heavy metals (e.g. Pt) and transition metal ferromagnets (e.g. Fe, Co, Ni) and their alloys have similar orders of magnitude, around or exceeding 10^3 S/cm. Taking a typical conductivity of $\sigma_{\mathrm{xx}} \sim (0.5 - 2) \times 10^4$ S/cm, the corresponding dimensionless spin-Hall ratio (or spin-Hall angle) $\theta_{\mathrm{SH}} = \sigma_{\mathrm{SH}}/\sigma_{\mathrm{xx}}$ is $\sim 0.05 - 0.2$, in line with experimental reports for metallic ferromagnets [65, 82–84]. Remarkably, other experiments have reported even higher values of spin-Hall ratios approaching unity in ferromagnets [85, 86]. Overall, we expect an appreciable spin-Hall current generated by the fixed magnetic layer.

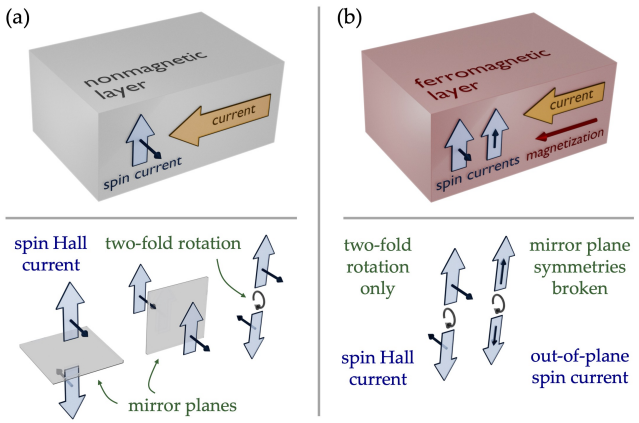

FIG. 2. Spin currents in nonmagnets and ferromagnets allowed by symmetry. (a) In bulk nonmagnetic materials under an applied electric field, spin currents satisfy the constraint that the flow direction, spin direction, and electric field are mutually orthogonal. These spin currents, which arise from the spin-Hall effect, are constrained because only this spin current orientation satisfies the crystal's mirror plane and rotational symmetries. (b) In bulk ferromagnetic materials, where the applied electric field and magnetization are parallel, the mirror plane symmetries are broken by the magnetization, lowering the symmetry and the constraints on spin currents. Thus, an additional spin current orientation is allowed, where the flow and spin directions are parallel to each other and orthogonal to the electric field and magnetization. In this paper, we focus on such spin currents within a magnetic heterostructure with out-of-plane flow and spin direction, called *out-of-plane spin currents* for short.

Due to the lower symmetry of ferromagnets as compared to normal metals, ferromagnets may generate spin currents with less constrained spin orientations, as illustrated in Fig. 2(b). In particular, when the magnetization and electric field are both parallel and in-plane, symmetry allows out-of-plane spin currents to be generated [38, 52, 55]. Such spin currents can arise from multiple microscopic mechanisms, including the spin-orbit precession effect [40, 43, 53–55], the magnetic spin-Hall effect [44–46], and spin swapping [40, 87, 88].

We assume that the fixed magnetic layer is the sole source of spin currents[3]. Both the spin-Hall current and the out-of-plane spin current are assumed to be present in the simulated device, as shown in Fig. 3(a). These two spin currents have the same out-of-plane flow direction but their spin orientations are orthogonal to each other, leading to a competition of applied torques on the free magnetic layer. The out-of-plane

torque is operative only in the bottom layer (i.e., closer to the fixed layer) of the synthetic antiferromagnet [66, 71]. This is reasonable considering the ∼1-nm dephasing length scale of the injected transverse spin current [72, 73].

[3] Note that both the spin-Hall current and out-of-plane spin current can exert self-torques on the ferromagnetic layer that generates them [21, 80, 89]. However, here we are interested in in the case where an out-of-plane spin current escapes the fixed layer and is absorbed in the free layer.

spin current tilts the free layer magnetizations out-of-plane and drives precession, while the spin-Hall current pulls the magnetization in-plane and can perturb the oscillations. The relative strengths of these two torques determine the proposed device's capability to exhibit coherent easy-plane precession.

Understanding the microscopic mechanisms responsible for out-of-plane spin currents is not within the scope of this work. Yet, notably, several theoretical predictions suggest that out-of-plane spin current conductivities are comparable to spin-Hall conductivities within ferromagnets. On the other hand, the efficiency of the out-of-plane spin current generation has yet to be quantified systematically in experiments. Some experiments report sufficient out-of-plane spin current generation from the magnetic fixed layer to switch a perpendicular magnetic free layer [55, 56]. Other experiments suggest that the out-of-spin current from a ferromagnet can be between ∼10% to ∼200% of the spin-Hall current [65]. Thus, given the uncertainty in the typical strength of out-of-plane spin current generation in ferromagnets and at ferromagnet/nonmagnet interfaces, we simulate various possibilities in this work, from entirely spin-Hall current injection to entirely out-of-plane spin current injection.

III. SIMULATION DESCRIPTION

Our simulations were performed using MuMax^3 [90], which calculates the time evolution of a magnetization texture by solving the Landau-Lifshitz-Gilbert (LLG) equation. The LLG equation is given by [91, 92]

$$\frac{d\hat{\mathbf{m}}}{dt} = \frac{-|\gamma|}{1+\alpha^2}\left(\hat{\mathbf{m}} \times \mathbf{B}_{\text{eff}} + \alpha \hat{\mathbf{m}} \times (\hat{\mathbf{m}} \times \mathbf{B}_{\text{eff}})\right) + \boldsymbol{\tau}_S, \quad (1)$$

where γ is the gyromagnetic ratio, α is the Gilbert damping parameter, $\hat{\mathbf{m}}$ is the magnetization direction, and $\mathbf{B}_{\text{eff}}$ is the effective magnetic field. To capture spin torques, we also include the term $\boldsymbol{\tau}_S$, given by Slonczewski [8, 93],

$$\boldsymbol{\tau}_S = \frac{g\mu_B J g(\theta)}{eM_{\text{sat}}(1+\alpha^2)d}\left(\alpha \hat{\mathbf{m}} \times \hat{\mathbf{p}} - \frac{1}{M_{\text{sat}}}\hat{\mathbf{m}} \times (\hat{\mathbf{m}} \times \hat{\mathbf{p}})\right), \quad (2)$$

where g is the Landé factor, μ_B is the Bohr magneton, J the charge current density, $\hat{\mathbf{p}}$ is the polarization direction of the injected spin current, and $g(\theta)$ [8] is given by

$$g(\theta) = -1 + (1+P)^3\left(\frac{3+\cos\theta}{4P^{3/2}}\right)^{-1}, \quad (3)$$

where θ is the angle between $\hat{\mathbf{m}}$ and $\hat{\mathbf{p}}$ and P is the polarization of the injected spin current[4].

[4] Here, P is equivalent to the spin-Hall ratio, i.e., the conversion efficiency of charge current to spin current. For simplicity, we set $P = 1$, but we later comment on the consequence of a more reasonable value of P, e.g., of order 0.1.

Figure 3(a) shows the relevant device geometry, where the magnetic fixed layer is a ferromagnet and the magnetic free "layer" is a synthetic antiferromagnet. The red arrows in the free layer represent the magnetization of the bottom layer of the synthetic antiferromagnet. Each ferromagnetic layer comprising the synthetic antiferromagnet has dimensions 1 µm × 1 µm × 2 nm, saturation magnetization 1000 kA/m, Gilbert damping parameter 0.01, and ferromagnetic exchange constant 20 pJ/m. The in-plane magnetocrystalline anisotropy is zero, a good approximation for practical sputter-grown polycrystalline magnetic films. The RKKY interlayer coupling strength between the two layers is -1 mJ/m^2. The injected spin current is simulated by including the Slonczewski term $\boldsymbol{\tau}_S$ in the bottom ferromagnetic layer only [66, 71]. To make the simulations less cumbersome, we do not explicitly include the fixed layer where the spin current is generated.

The swept parameters are the total spin current density (j_s) and the ratio (β) of out-of-plane spin current density j_s^{OOP} to the total spin current density given by

$$j_s = \sqrt{(j_s^{\text{SHE}})^2 + (j_s^{\text{OOP}})^2} \quad (4)$$

$$\beta = j_s^{\text{OOP}}/j_s. \quad (5)$$

Assuming the electric field (charge current) points along $\hat{\mathbf{x}}$, the spin-Hall current j_s^{SHE} has an in-plane spin polarization along $\hat{\mathbf{y}}$. The out-of-plane spin current j_s^{OOP} by definition has a spin polarization along $\hat{\mathbf{z}}$. Thus, the polarization direction $\hat{\mathbf{p}}$ of the injected spin current lies within the yz-plane, where $\arcsin(\beta)$ is the angle between $\hat{\mathbf{p}}$ and $\hat{\mathbf{y}}$. Thus, β determines the polarization angle and j_s determines the magnitude of the injected spin current.

The effects of temperature is included by adding a stochastic thermal field to the effective field ($\mathbf{B}_{\text{eff}}$) in the LLG equation [94]. The stochastic thermal field is given by [90, 94, 95]

$$\mathbf{B}_{\text{therm}} = \boldsymbol{\eta}_{\text{step}}\sqrt{\frac{2\mu_0\alpha k_B T}{B_{\text{sat}}\Delta V \Delta t}}, \quad (6)$$

where α is the damping parameter, k_B is the Boltzmann constant, T is the temperature, $B_{\text{sat}} = \mu_0 M_s$ is the saturation magnetic field, ΔV is the cell volume, Δt is the simulation time step, and $\boldsymbol{\eta}_{\text{step}}$ is a random vector determined via a standard normal distribution.

IV. RESULTS

To confirm GHz steady-state oscillations in the free layer, simulations were run to 1 µs to capture several hundred periods. Figure 3(b) shows the oscillation frequency of magnetic free layer as a function of j_s and β. We choose spin current densities j_s on the order of 10^{11} A/m^2, which are consistent with other micromagnetic simulations of spin-orbit torque oscillators [96]. The in-plane electric charge current density to drive the

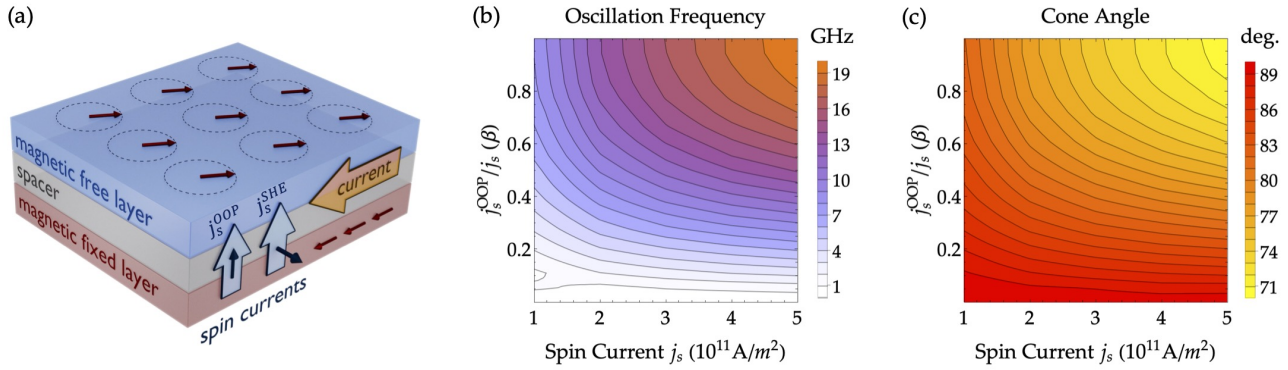

FIG. 3. (a) The proposed device, where the magnetic fixed layer is a ferromagnet and the magnetic free layer is a synthetic antiferromagnet. Red arrows in the fixed layer depict the fixed magnetization while red arrows in the free layer depict the bottom layer magnetization of the synthetic antiferromagnet. Under an applied, in-plane electric field, the fixed layer generates both a spin-Hall current density $j_s^{\rm SHE}$ and an out-of-plane spin current density $j_s^{\rm OOP}$. (b) Contour plot of the oscillation frequency of the magnetic free layer as a function or the total spin current density j_s and the spin current ratio β, defined in Eqs. (4) and (5). (c) Contour plot of the cone angle of oscillation as a function of the same parameters as in panel (b). Self-sustained oscillations occur over the majority of the parameter space, with the oscillator failing for $\beta \lesssim 0.1$.

device is $j_c = \theta_{\rm SH} j_s$. Taking a conservative spin-Hall ratio of $\theta_{\rm SH} \sim 0.1$ for the fixed magnetic layer (see Sec. II B), the charge current densities could be as high as $j_c \sim 10^{12}$ A/m^2. This charge current density is typical for experimentally demonstrated spin-orbit torque oscillators [25, 26, 32, 35, 36]. However, a charge current density much lower than 10^{12} A/m^2 is desirable for reducing power dissipation and detrimental heating. We give further consideration to this issue in Sec. V.

As the spin current ratio β is swept from 0 to 1, the injected spin current changes from entirely spin-Hall current $\beta = 0$ to entirely out-of-plane spin current $\beta = 1$. The results shown in Fig. 3(b) confirm the trend that increasing j_s or β increases the oscillation frequency. This trend can be understood as follows. Increasing j_s or β will increase the injected out-of-plane spin current (unless $\beta = 0$), which further tilts the free-layer magnetization out-of-plane. As the tilt angle increases, so does the torque provided by the internal field, which in turn increases the frequency of oscillation. To achieve the highest oscillation frequency within the range of parameters studied, j_s and β should be maximized.

Figure 3(c) shows the time-averaged cone angle $\theta_{\rm c}$ of magnetic free layer as a function of j_s and β. Note that a time-averaged cone angle of $\theta_{\rm c} = 90°$ corresponds to fully in-plane oscillations. The precessing magnetization generates an oscillating voltage output from the swinging resistance, due to the giant magnetoresistance of the spin valve. In particular, as the free-layer magnetization (in the bottom layer of the synthetic antiferromagnet, closer to the fixed layer) rotates from being parallel to antiparallel to the fixed-layer magnetization, the resistance swings from its low state to high state [66, 97]. The magnitude of the oscillating signal output is proportional to the in-plane component of the precessing magnetization – i.e., $\sin\theta_{\rm c}$, maximized at $\theta_{\rm c} = 90°$. By increasing the out-of-plane spin current density, the magnetization tilts further out-of-plane and the time-averaged cone angle decreases. Nevertheless, within our simulated parameter space, the cone angle remains large at $\theta_{\rm c} \gtrsim 70°$. The corresponding magnetization remains mostly in-plane ($\sin\theta_{\rm c} \gtrsim 0.9$) such that the magnetoresistance signal output remains large.

In Fig. 4, we plot the time evolution of the magnetization direction $\hat{\mathbf{m}}$ at $j_s = 3 \times 10^{11}$A/m^2 for both $T = 0$ K and $T = 300$ K and for both $\beta = 0.08$ (mostly spin-Hall current injection) and $\beta = 1$ (entirely out-of-plane spin current injection). The magnetization plotted corresponds to the bottom layer of the synthetic antiferromaget. Panels (a) and (d) show that in all cases, the magnetization sweeps a nearly circular path in the xy-plane (i.e. in-plane).

The results shown in Fig. 3 and Fig. 4 indicate that large cone-angle, self-sustained GHz oscillations occur in the proposed device over a wide parameter space. Panels (b) and (e) in Fig. 4 highlight the primary effect of temperature, which is to introduce fluctuations in the out-of-plane component of the magnetization, m_z. The fluctuations in the in-plane magnetization components, m_x and m_y, are only a few percent of the easy-plane precession amplitude. Thus, the thermal fluctuations do not significantly affect the swing in resistance (output voltage) determined by m_x and m_y.

We now discuss the threshold regime in which easy-plane self-oscillations emerge at small β of $\sim$0.1. The out-of-plane spin currents corresponding to such β values are about one order of magnitude less than the spin-Hall currents, well within theoretical predictions [43, 46]. To study this threshold regime, we performed additional simulations for small β values from 0 to 0.14 in increments of 0.02. As β approaches zero, the out-of-

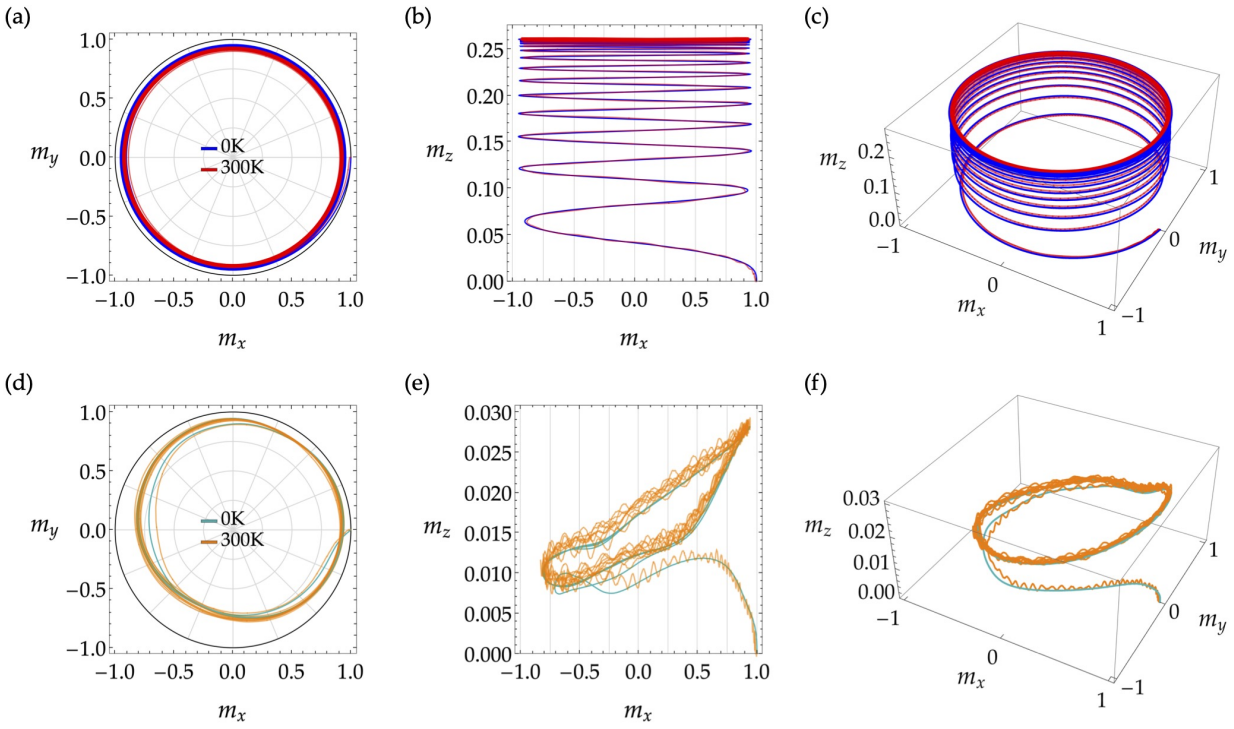

FIG. 4. Trajectories of magnetization direction of one layer in the synthetic antiferromagnet free layer over the unit sphere at absolute zero and at room temperature. The top row panels correspond to $\beta = 1$, that is, the injected spin current from the fixed layer is entirely the out-of-plane spin current. The bottom row panels correspond to $\beta = 0.08$, where the injected spin currents consist of mostly the spin-Hall current. Panels (a) and (d) show the time evolution of the in-plane (i.e. x and y) magnetization components, while panels (b) and (e) show the x and z components. Panels (c) and (f) are three-dimensional plots of the same trajectories as (a,b) and (d,e). Panels (a) and (d) show that regardless of temperature and ratio of out-of-plane spin current to spin-Hall current, self-sustained oscillations occur with large cone angle (i.e. with the magnetization mostly in-plane). Panels (b) and (e) show that the effect of temperature is most prominent for low β values, and leads to noise in the z component of the magnetization, which has minimal effect on the primary oscillation output signal (xy component of the magnetization).

plane spin current contribution vanishes, leaving only the spin-Hall current. In this regime, we do not expect easy-plane oscillations to occur, since the out-of-plane spin current is required to tilt the magnetization out-of-plane and induce self-sustained oscillations about the internal field. In Fig. 5(a)-(b), we show the oscillation frequency as a function of β and j_s for (a) 0 K and (b) 300 K in the threshold regime. In both cases, self-sustained oscillations persist for β values approaching 0.04, which suggests that the out-of-plane spin current can be as low as 4% of the spin-Hall current and still create self-sustained oscillations.

Figure 5(c) shows the x-component of magnetization plotted versus time to further illustrate dynamics in the threshold regime. While small β values can introduce higher-order harmonics, as seen in the plot for $\beta = 0.061$, self-sustained oscillations with large cone angle still persist. At $\beta = 0.123$, higher-order harmonics vanish; such clean sinusoidal oscillations arise from a circular orbit of easy-plane magnetic precession (see Fig. 3(a-c)). Our simulation results indicate that coherent easy-plane precession can be stabilized even at small β, i.e., when the out-of-plane spin current is only ∼10% of the spin-Hall current. This finding is highly encouraging for realizing large-amplitude, easy-plane spin-orbit torque oscillators under realistic conditions.

V. IMPLICATIONS FOR APPLICATIONS

Easy-plane spin-orbit torque oscillators in general exhibit a circular precessional orbit with a large cone angle approaching 90°. These features lead to a larger signal output and higher stability against magnon scattering [35, 98] compared to conventional spin-orbit torque oscillators with a small cone-angle, elliptical precessional orbit. The easy-plane oscillators are promising for applications in neuromorphic computing [27–29] and may be applied to magnetic devices that mimic Josephson junctions [63, 99].

Other proposals of easy-plane spin-orbit torque oscillators [27, 28, 63] rely on the anti-damping spin-

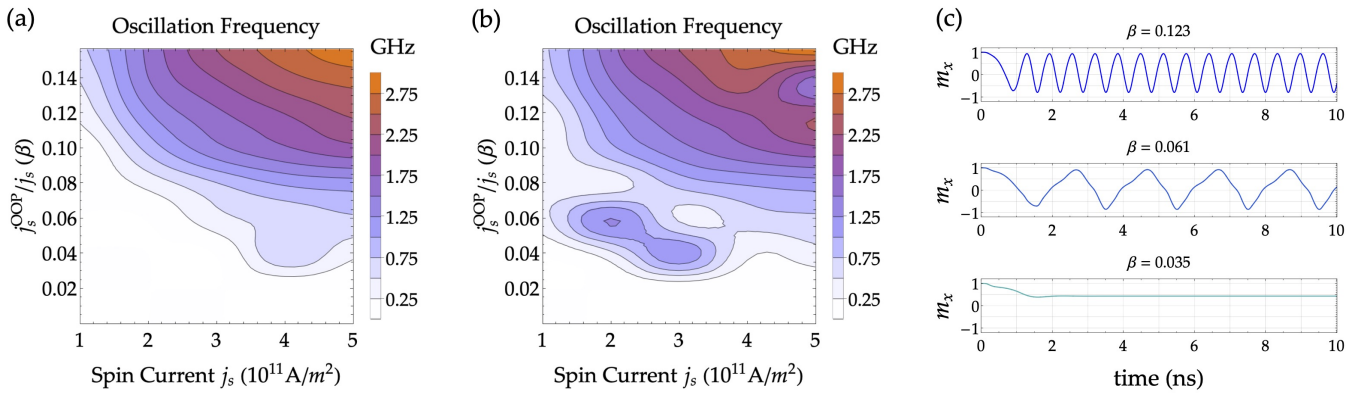

FIG. 5. Threshold regime with low β in which self-sustained oscillations emerge. Panel (a) plots oscillation frequency at $T = 0$ K as a function of j_s and β. Panel (b) is the same as panel (a) but for $T = 300$ K. Panel (c) shows the time evolution of m_x (corresponding to the synthetic antiferromagnet's bottom layer) for $j_s = 3\times10^{11}$A/m^2 for various small β values. Self-sustained oscillations persist even if the out-of-plane spin current is roughly an order of magnitude less than the spin-Hall current.

orbit torque driven by spin-Hall spin current. Hence, the precessional axis is in-plane transverse to the current axis. To achieve a circular, large-cone-angle precessional orbit, careful tuning of magnetic anisotropy is required. For example, the experimental demonstrations so far [29, 35, 98] attain easy-plane precession in Co/Ni multilayers with perpendicular magnetic anisotropy, precisely tuned to counterbalance the out-of-plane magnetic shape anisotropy. This approach limits the choices of materials for the free layer, making it difficult to lower damping and enhance magnetoresistance for practical devices.

In our proposed oscillator driven by out-of-plane spin current, the out-of-plane internal field (e.g., demagnetization field) defines the precessional axis. Hence, the precession is within the film plane – the natural easy plane for soft ferromagnetic metal films governed by shape anisotropy. No particular engineering of perpendicular magnetic anisotropy is needed, so various materials may be employed to optimize the performance of the oscillator. For instance, Ni-Fe and Fe-V alloys [84, 100–102] with low damping and low saturation magnetization may be a good choice to reduce the threshold current density to drive precessional dynamics. Moreover, our proposed oscillator is essentially based on a current-in-plane spin valve with giant magnetoresistance. Such film heterostructures already find wide usage in commercial sensors and are therefore more amenable to practical applications. The oscillators can then leverage established materials optimization approaches. For example, the giant magnetoresistance ratio may be enhanced to ∼10% – much greater than the anisotropic magnetoresistance ratio of ∼1% typical for spin-orbit torque oscillators – with subnanometer interfacial dusting layers [103] and encapsulation with insulating layers [104]. Overall, our proposed scheme is highly promising for broad materials options and compatibility with common device fabrication protocols.

The biggest practical challenge is to realize a sufficient out-of-plane spin current from the fixed-layer ferromagnet. In a recent experiment, the out-of-plane spin current was reported to switch perpendicular magnetization in a "T-type" current-in-plane spin valve (in-plane fixed layer, out-of-plane free layer) [55, 56]. Yet, an experimental report of the out-of-plane spin current tuning or triggering precessional magnetization dynamics is still lacking. Symmetry guarantees the emergence of an out-of-plane spin current from an in-plane magnetized ferromagnet [38, 52, 55]. The question is whether the magnitude of the out-of-plane spin current can become large enough, particularly under a reasonably low charge current. As discussed in Sec. III, taking a reasonable spin-Hall ratio is of order 0.1 in ferromagnetic metals [65, 82–84], the required charge-current density would be $\sim10^{12}$ A/m^2. Although such a current density j_c is common for existing nano-scale spin-orbit torque oscillators, the larger cross-sectional area A of our proposed oscillator would necessitate a larger drive current $I_c = j_c A$. The large I_c could be problematic because the power dissipation (Joule heating) scales as ${I_c}^2$; in addition to deteriorating the power efficiency, excessive heating could damage the device.

For real applications, it is desirable to reduce the charge current density by about an order of magnitude to $\sim10^{11}$ A/m^2. Thus, experimental endeavors should enhance the spin-Hall ratio in ferromagnetic metals for the fixed layer, preferably to $\gtrsim$0.3. Giant spin-Hall ratios have been claimed in some ferromagnetic metals [85, 86], but further work is required to verify and tailor ferromagnets with simultaneously large spin-Hall and giant magnetoresistance ratios. Another approach is to increase the ratio of the out-of-plane to in-plane spin current. Some experimental work claims out-of-plane to in-plane spin current ratios exceeding ∼200% [65], though refinement in experimental quantification may be warranted. Further enhancements may be feasible by

incorporating elements with strong spin-orbit coupling (e.g., Pt, Ir, rare-earth metals) into the fixed-layer ferromagnet [105]. Yet another possibility is to leverage antiferromagnets with strong spin-orbit effects as an alternative to the ferromagnetic fixed layer. For instance, recent experiments point to IrMn, a widely used antiferromagnetic alloy for exchange-biasing spin valves, as a robust source of out-of-plane spin current [106, 107].

Finally, while we expect damping-like torques to primarily influence the magnetization dynamics of the proposed oscillators, field-like torques could modulate the precession frequencies and ellipticities. The strength of field-like torques from spin current absorption at a nonmagnet/ferromagnet interface is determined in part by the imaginary part of the spin mixing conductance. Since the ratio of the imaginary part to the real part of the spin mixing conductance is minimal in the relevant material systems [108], we do not expect such field-like torques to play a strong role. Field-like torques could also arise from inverse spin galvanic effects at the interface between the spacer layer and the bottom layer of the synthetic antiferromagnet. Such field-like torques are typically small at interfaces between typical spacer layer materials like Cu or Ti and ferromagnetic materials like CoFeB or NiFe. In trilayers, large field-like torques have been reported [52] and are possibly related to a combination of interlayer scattering and spin-orbit effects [109, 110]; however, these field-like torques are appreciable only when the fixed layer magnetization is perpendicular to the free layer magnetization's plane of rotation, which is not the case here.

VI. OUTLOOK AND CONCLUSIONS

Using micromagnetic simulations, we have demonstrated that self-sustained, large-amplitude GHz oscillations are feasible in spin-orbit torque oscillators without an external bias magnetic field. The spin-orbit torque oscillator consists of a fixed ferromagnetic layer, a spacer layer, and a synthetic antiferromagnet as the magnetic free layer, the latter of which is required to obtain coherent oscillations. The oscillator is driven by an in-plane current, which generates various spin currents in the fixed ferromagnetic layer that flow out-of-plane and exert torques on the magnetic free layer. Oscillations occur about an internal effective field rather than an external magnetic field, with the spin-orbit torque counteracting the damping torque in the free layer. To address the uncertainty in the strength of the relevant spin currents in realistic materials, we have varied the ratio of the out-of-plane spin current to the spin-Hall current in our simulations, and found that self-sustained oscillations occur even if the out-of-plane spin current is as low as 4% of the spin-Hall current. The robust performance of these spin-orbit torque oscillators at room temperature presents intriguing possibilities for future spintronic devices with possible applications to microwave communications and neuromorphic computing.

ACKNOWLEDGMENTS

T.N. was supported by the National Science Foundation under Grant No. DMR-2105219. V.P.A was supported by the National Science Foundation under grant ECCS-2236159. D.A.S. and F.R.-D. were supported by the National Science Foundation under Grant No. DMR-2003914. S.E. was supported by the National Science Foundation under Grant No. ECCS-2236160.

[1] N. Locatelli, V. Cros, and J. Grollier, Spin-torque building blocks, Nature Materials **13**, 11 (2014).
[2] J. Grollier, D. Querlioz, and M. D. Stiles, Spintronic nanodevices for bioinspired computing, Proceedings of the IEEE **104**, 2024 (2016).
[3] H. Lim, S. Ahn, M. Kim, S. Lee, and H. Shin, A new circuit model for spin-torque oscillator including perpendicular torque of magnetic tunnel junction, Advances in Condensed Matter Physics **2013** (2013).
[4] D. Houssameddine, U. Ebels, B. Delaët, B. Rodmacq, I. Firastrau, F. Ponthenier, M. Brunet, C. Thirion, J.-P. Michel, L. Prejbeanu-Buda, M.-C. Cyrille, O. Redon, and B. Dieny, Spin-torque oscillator using a perpendicular polarizer and a planar free layer, Nature Materials **6**, 447 (2007).
[5] R. E. Troncoso, K. Rode, P. Stamenov, J. M. D. Coey, and A. Brataas, Antiferromagnetic single-layer spin-orbit torque oscillators, Phys. Rev. B **99**, 054433 (2019).
[6] W. H. Rippard, M. R. Pufall, S. Kaka, S. E. Russek, and T. J. Silva, Direct-current induced dynamics in $co_{90}fe_{10}/ni_{80}fe_{20}$ point contacts, Phys. Rev. Lett. **92**, 027201 (2004).
[7] S. I. Kiselev, J. C. Sankey, I. N. Krivorotov, N. C. Emley, R. J. Schoelkopf, R. A. Buhrman, and D. C. Ralph, Microwave oscillations of a nanomagnet driven by a spin-polarized current, Nature **425**, 380 (2003).
[8] J. C. Slonczewski, Current-driven excitation of magnetic multilayers, Journal of Magnetism and Magnetic Materials **159**, L1 (1996).
[9] M. D. Stiles and A. Zangwill, Anatomy of spin-transfer torque, Phys. Rev. B **66**, 014407 (2002).
[10] M. Tsoi, A. G. M. Jansen, J. Bass, W.-C. Chiang, M. Seck, V. Tsoi, and P. Wyder, Excitation of a magnetic multilayer by an electric current, Phys. Rev. Lett. **80**, 4281 (1998).
[11] M. Tsoi, A. G. M. Jansen, J. Bass, W.-C. Chiang, V. Tsoi, and P. Wyder, Generation and detection

of phase-coherent current-driven magnons in magnetic multilayers, Nature **406**, 46 (2000).
[12] J. A. Katine, F. J. Albert, R. A. Buhrman, E. B. Myers, and D. C. Ralph, Current-driven magnetization reversal and spin-wave excitations in co /cu /co pillars, Phys. Rev. Lett. **84**, 3149 (2000).
[13] W. H. Rippard, M. R. Pufall, S. Kaka, S. E. Russek, and T. J. Silva, Direct-current induced dynamics in $co_{90}fe_{10}/ni_{80}fe_{20}$ point contacts, Phys. Rev. Lett. **92**, 027201 (2004).
[14] G. D. Fuchs, N. C. Emley, I. N. Krivorotov, P. M. Braganca, E. M. Ryan, S. I. Kiselev, J. C. Sankey, D. C. Ralph, R. A. Buhrman, and J. A. Katine, Spin-transfer effects in nanoscale magnetic tunnel junctions, Applied Physics Letters **85**, 1205 (2004).
[15] H. Maehara, H. Kubota, Y. Suzuki, T. Seki, K. Nishimura, Y. Nagamine, K. Tsunekawa, A. Fukushima, A. M. Deac, K. Ando, and S. Yuasa, Large emission power over 2 µw with high q factor obtained from nanocontact magnetic-tunnel-junction-based spin torque oscillator, Applied Physics Express **6**, 113005 (2013).
[16] A. Houshang, R. Khymyn, H. Fulara, A. Gangwar, M. Haidar, S. R. Etesami, R. Ferreira, P. P. Freitas, M. Dvornik, R. K. Dumas, and J. Åkerman, Spin transfer torque driven higher-order propagating spin waves in nano-contact magnetic tunnel junctions, Nature Communications **9**, 4374 (2018).
[17] C. Yoshida, M. Kurasawa, Y. M. Lee, K. Tsunoda, M. Aoki, and Y. Sugiyama, A study of dielectric breakdown mechanism in cofeb/mgo/cofeb magnetic tunnel junction, in *2009 IEEE International Reliability Physics Symposium* (2009) pp. 139–142.
[18] T. Chen, R. K. Dumas, A. Eklund, P. K. Muduli, A. Houshang, A. A. Awad, P. Dürrenfeld, B. G. Malm, A. Rusu, and J. Åkerman, Spin-torque and spin-hall nano-oscillators, Proceedings of the IEEE **104**, 1919 (2016).
[19] R. K. Dumas, E. Iacocca, S. Bonetti, S. R. Sani, S. M. Mohseni, A. Eklund, J. Persson, O. Heinonen, and J. Åkerman, Spin-wave-mode coexistence on the nanoscale: A consequence of the oersted-field-induced asymmetric energy landscape, Phys. Rev. Lett. **110**, 257202 (2013).
[20] W. H. Rippard, M. R. Pufall, and S. E. Russek, Comparison of frequency, linewidth, and output power in measurements of spin-transfer nanocontact oscillators, Physical Review B **74**, 224409 (2006).
[21] A. Hoffmann, Spin hall effects in metals, IEEE Transactions on Magnetics **49**, 5172 (2013).
[22] J. Sinova, S. O. Valenzuela, J. Wunderlich, C. H. Back, and T. Jungwirth, Spin hall effects, Reviews of Modern Physics **87**, 1213 (2015).
[23] A. Manchon, J. Železný, I. M. Miron, T. Jungwirth, J. Sinova, A. Thiaville, K. Garello, and P. Gambardella, Current-induced spin-orbit torques in ferromagnetic and antiferromagnetic systems, Reviews of Modern Physics **91**, 035004 (2019).
[24] L. Liu, C.-F. Pai, D. C. Ralph, and R. A. Buhrman, Magnetic oscillations driven by the spin hall effect in 3-terminal magnetic tunnel junction devices, Physical Review Letters **109**, 186602 (2012).
[25] A. A. Awad, P. Dürrenfeld, A. Houshang, M. Dvornik, E. Iacocca, R. K. Dumas, and J. Åkerman, Long-range mutual synchronization of spin hall nano-oscillators, Nature Physics **12**, 292–299 (2017).
[26] M. Zahedinejad, A. A. Awad, S. Muralidhar, R. Khymyn, H. Fulara, H. Mazraati, M. Dvornik, and J. Åkerman, wo-dimensional mutually synchronized spin hall nano-oscillator arrays for neuromorphic computing, Nature Nanotechnology **15**, 47–52 (2020).
[27] D. Marković, M. W. Daniels, P. Sethi, A. D. Kent, M. D. Stiles, and J. Grollier, Easy-plane spin hall nano-oscillators as spiking neurons for neuromorphic computing, Phys. Rev. B **105**, 014411 (2022).
[28] S. Manna, R. Medwal, and R. S. Rawat, Reconfigurable neural spiking in bias field free spin hall nano-oscillator, Physical Review B **108**, 184411 (2023).
[29] P. Sethi, D. Sanz-Hernández, F. Godel, S. Krishnia, F. Ajejas, A. Mizrahi, V. Cros, D. Marković, and J. Grollier, Compensation of anisotropy in spin hall devices for neuromorphic applications, Physical Review Applied **19**, 064018 (2023).
[30] R. L. Stamps, S. Breitkreutz, J. Åkerman, A. V. Chumak, Y. Otani, G. E. W. Bauer, J.-U. Thiele, M. Bowen, S. A. Majetich, M. Kläui, I. L. Prejbeanu, B. Dieny, N. M. Dempsey, and B. Hillebrands, The 2014 magnetism roadmap, Journal of Physics D: Applied Physics **47**, 333001 (2014).
[31] M. Haidar, H. Mazraati, P. Dürrenfeld, H. Fulara, M. Ranjbar, and J. Åkerman, Compositional effect on auto-oscillation behavior of $ni_{100-x}fe_x$/pt spin hall nano-oscillators, Applied Physics Letters **118**, 12406 (2021).
[32] Z. Duan, A. Smith, L. Yang, B. Youngblood, J. Lindner, V. E. Demidov, S. O. Demokritov, and I. N. Krivorotov, Nanowire spin torque oscillator driven by spin orbit torques, Nature Communications **5**, 5616 (2014).
[33] V. E. Demidov, S. Urazhdin, E. R. J. Edwards, M. D. Stiles, R. D. McMichael, and S. O. Demokritov, Control of magnetic fluctuations by spin current, Physical Review Letters **107**, 107204 (2011).
[34] M. Dvornik, A. A. Awad, and J. Åkerman, Origin of magnetization auto-oscillations in constriction-based spin hall nano-oscillators, Phys. Rev. Appl. **9**, 014017 (2018).
[35] B. Divinskiy, S. Urazhdin, S. O. Demokritov, and V. E. Demidov, Controlled nonlinear magnetic damping in spin-hall nano-devices, Nature Communications **10**, 5211 (2019).
[36] V. E. Demidov, S. Urazhdin, A. Zholud, A. V. Sadovnikov, and S. O. Demokritov, Nanoconstriction-based spin-hall nano-oscillator, Applied Physics Letters **105**, 172410 (2014).
[37] A. Kumar, H. Fulara, R. Khymyn, A. Litvinenko, M. Zahedinejad, M. Rajabali, X. Zhao, N. Behera, A. Houshang, A. A. Awad, and J. Åkerman, Robust mutual synchronization in long spin hall nano-oscillator chains, Nano Letters **23**, 6720 (2023), pMID: 37450893.
[38] M. Seemann, D. Ködderitzsch, S. Wimmer, and H. Ebert, Symmetry-imposed shape of linear response tensors, Phys. Rev. B **92**, 155138 (2015).
[39] A. Davidson, V. P. Amin, W. S. Aljuaid, P. M. Haney, and X. Fan, Perspectives of electrically generated spin currents in ferromagnetic materials, Physics Letters A **384**, 126228 (2020).

[40] V. P. Amin, P. M. Haney, and M. D. Stiles, Interfacial spinÄìorbit torques, Journal of Applied Physics **128**, 151101 (2020).

[41] V. P. Amin and M. D. Stiles, Spin transport at interfaces with spin-orbit coupling: Phenomenology, Phys. Rev. B **94**, 104420 (2016).

[42] V. P. Amin and M. D. Stiles, Spin transport at interfaces with spin-orbit coupling: Formalism, Phys. Rev. B **94**, 104419 (2016).

[43] V. P. Amin, J. Zemen, and M. D. Stiles, Interface-generated spin currents, Phys. Rev. Lett. **121**, 136805 (2018).

[44] A. Mook, R. R. Neumann, A. Johansson, J. Henk, and I. Mertig, Origin of the magnetic spin hall effect: Spin current vorticity in the fermi sea, Phys. Rev. Res. **2**, 023065 (2020).

[45] K.-W. Kim and K.-J. Lee, Generalized spin drift-diffusion formalism in the presence of spin-orbit interaction of ferromagnets, Phys. Rev. Lett. **125**, 207205 (2020).

[46] L. Salemi and P. M. Oppeneer, Theory of magnetic spin and orbital hall and nernst effects in bulk ferromagnets, Phys. Rev. B **106**, 024410 (2022).

[47] D. MacNeill, G. M. Stiehl, M. H. D. Guimaraes, R. A. Buhrman, J. Park, and D. C. Ralph, Control of spin–orbit torques through crystal symmetry in wte2/ferromagnet bilayers, Nature Physics **13**, 300 (2017).

[48] P. Gupta, N. Chowdhury, M. Xu, P. K. Muduli, A. Kumar, K. Kondou, Y. Otani, and P. K. Muduli, Generation of out-of-plane polarized spin current in (permalloy, cu)/eus interfaces, Phys. Rev. B **109**, L060405 (2024).

[49] L. Bainsla, B. Zhao, N. Behera, A. M. Hoque, L. Sjöström, A. Martinelli, M. Abdel-Hafiez, J. Åkerman, and S. P. Dash, Large out-of-plane spin-orbit torque in topological weyl semimetal tairte4, Nature Communications **15**, 4649 (2024).

[50] Q. Liu, X. Lin, A. Shaked, Z. Nie, G. Yu, and L. Zhu, Efficient generation of out-of-plane polarized spin current in polycrystalline heavy metal devices with broken electric symmetries, Advanced Materials **36**, 2406552 (2024).

[51] S. M, S. Srivatsava, S. Panwar, V. Nehra, R. Kamal, and A. Acharya, Impact of unconventional torque on the performance of weyl-semimetal-based sot-mtj: A micromagnetic study, IEEE Transactions on Electron Devices **71**, 2177 (2024).

[52] A. M. Humphries, T. Wang, E. R. J. Edwards, S. R. Allen, J. M. Shaw, H. T. Nembach, J. Q. Xiao, T. J. Silva, and X. Fan, Observation of spin-orbit effects with spin rotation symmetry, Nature Communications **8**, 911 (2017).

[53] Y. Hibino, K. Hasegawa, T. Koyama, and D. Chiba, Spin-orbit torque generated by spin-orbit precession effect in Py/Pt/Co tri-layer structure, APL Materials **8**, 041110 (2020).

[54] W. Wang, Q. Fu, K. Zhou, L. Chen, L. Yang, Z. Li, Z. Tao, C. Yan, L. Liang, X. Zhan, Y. Du, and R. Liu, Unconventional spin currents generated by the spin-orbit precession effect in perpendicularly magnetized Co−Tb ferrimagnetic system, Phys. Rev. Appl. **17**, 034026 (2022).

[55] S.-h. C. Baek, V. P. Amin, Y.-W. Oh, G. Go, S.-J. Lee, G.-H. Lee, K.-J. Kim, M. D. Stiles, B.-G. Park, and K.-J. Lee, Spin currents and spin–orbit torques in ferromagnetic trilayers, Nature Materials **17**, 509 (2018).

[56] M. Yang, L. Sun, Y. Zeng, J. Cheng, K. He, X. Yang, Z. Wang, L. Yu, H. Niu, T. Ji, G. Chen, B. Miao, X. Wang, and H. Ding, Highly efficient field-free switching of perpendicular yttrium iron garnet with collinear spin current, Nat. Commun. **15**, 3201 (2024).

[57] S. Liang, A. Chen, L. Han, H. Bai, C. Chen, L. Huang, M. Ma, F. Pan, X. Zhang, and C. Song, Field-free perpendicular magnetic memory driven by out-of-plane spin-orbit torques, Advanced Functional Materials **n/a**, 2417731 (2024).

[58] D. A. Smith, S. Takei, B. Brann, L. Compton, F. Ramos-Diaz, M. J. Simmers, and S. Emori, Diffusive and fluidlike motion of homochiral domain walls in easy-plane magnetic strips, Phys. Rev. Applied **16**, 054002 (2021).

[59] E. B. Sonin, Spin currents and spin superfluidity, Advances in Physics **59**, 181 (2010).

[60] S. Takei and Y. Tserkovnyak, Superfluid spin transport through easy-plane ferromagnetic insulators, Physical Review Letters **112**, 227201 (2014).

[61] H. Skarsvåg, C. Holmqvist, and A. Brataas, Spin superfluidity and long-range transport in thin-film ferromagnets, Phys. Rev. Lett. **115**, 237201 (2015).

[62] E. Iacocca and M. A. Hoefer, Perspectives on spin hydrodynamics in ferromagnetic materials, Physics Letters A , 125858 (2019).

[63] Y. Liu, I. Barsukov, Y. Barlas, I. N. Krivorotov, and R. K. Lake, Synthetic antiferromagnet-based spin josephson oscillator, Applied Physics Letters **116**, 132409 (2020).

[64] A. Shadman and J.-G. Zhu, Micromagnetic insights on in-plane magnetization rotation and propagation of magnetization waves in nanowires, Scientific Reports **13**, 13438 (2023).

[65] Q. Fu, L. Liang, W. Wang, L. Yang, K. Zhou, Z. Li, C. Yan, L. Li, H. Li, and R. Liu, Observation of nontrivial spin-orbit torque in single-layer ferromagnetic metals, Phys. Rev. B **105**, 224417 (2022).

[66] I. Volvach, A. D. Kent, E. E. Fullerton, and V. Lomakin, Spin-transfer-torque oscillator with an antiferromagnetic exchange-coupled composite free layer, Phys. Rev. Applied **18**, 024071 (2022).

[67] R. Duine, K. Lee, S. Parkin, and M. Stiles, Synthetic antiferromagnetic spintronics, Nature Physics **14**, 217–219 (2018).

[68] S. Lepadatu, H. Saarikoski, R. Beacham, M. J. Benitez, T. A. Moore, G. Burnell, S. Sugimoto, D. Yesudas, M. C. Wheeler, J. Miguel, S. S. Dhesi, D. McGrouther, S. McVitie, G. Tatara, and C. H. Marrows, Synthetic ferrimagnet nanowires with very low critical current density for coupled domain wall motion, Sci. Rep. **7**, 1640 (2017).

[69] Y. Zhou, C. L. Zha, S. Bonetti, J. Persson, and J. Åkerman, Microwave generation of tilted-polarizer spin torque oscillator, Journal of Applied Physics **105**, 07D116 (2009).

[70] D. Houssameddine, J. F. Sierra, D. Gusakova, B. Delaet, U. Ebels, L. D. Buda-Prejbeanu, M.-C. Cyrille, B. Dieny, B. Ocker, J. Langer, and W. Maas, Spin

torque driven excitations in a synthetic antiferromagnet, Applied Physics Letters **96**, 072511 (2010).
[71] I. Firastrau, L. D. Buda-Prejbeanu, B. Dieny, and U. Ebels, Spin-torque nano-oscillator based on a synthetic antiferromagnet free layer and perpendicular to plane polarizer, Journal of Applied Physics **113**, 113908 (2013).
[72] A. Ghosh, S. Auffret, U. Ebels, and W. E. Bailey, Penetration depth of transverse spin current in ultrathin ferromagnets, Phys. Rev. Lett. **109**, 127202 (2012).
[73] Y. Lim, S. Wu, D. A. Smith, C. Klewe, P. Shafer, and S. Emori, Absorption of transverse spin current in ferromagnetic NiCu: Dominance of bulk dephasing over spin-flip scattering, Appl. Phys. Lett. **121**, 222403 (2022).
[74] J. E. Hirsch, Spin hall effect, Phys. Rev. Lett. **83**, 1834 (1999).
[75] V. P. Amin, J. Li, M. D. Stiles, and P. M. Haney, Intrinsic spin currents in ferromagnets, Phys. Rev. B **99**, 220405 (2019).
[76] Y. Miura and K. Masuda, First-principles calculations on the spin anomalous hall effect of ferromagnetic alloys, Phys. Rev. Mater. **5**, L101402 (2021).
[77] F. Zheng, M. Zhu, J. Dong, X. Li, Y. Zhou, K. Wu, and J. Zhang, Anatomy of the spin hall effect in ferromagnetic metals, Phys. Rev. B **109**, 224401 (2024).
[78] D. Tian, Y. Li, D. Qu, S. Y. Huang, X. Jin, and C. L. Chien, Manipulation of pure spin current in ferromagnetic metals independent of magnetization, Phys. Rev. B **94**, 020403 (2016).
[79] K. S. Das, W. Y. Schoemaker, B. J. van Wees, and I. J. Vera-Marun, Spin injection and detection via the anomalous spin hall effect of a ferromagnetic metal, Phys. Rev. B **96**, 220408 (2017).
[80] W. Wang, T. Wang, V. P. Amin, Y. Wang, A. Radhakrishnan, A. Davidson, S. R. Allen, T. J. Silva, H. Ohldag, D. Balzar, B. L. Zink, P. M. Haney, J. Q. Xiao, D. G. Cahill, V. O. Lorenz, and X. Fan, Anomalous spin–orbit torques in magnetic single-layer films, Nature Nanotechnology **14**, 819 (2019).
[81] N. Soya, M. Yamada, K. Hamaya, and K. Ando, Isotropic spin hall effect in an epitaxial ferromagnet, Phys. Rev. Lett. **131**, 076702 (2023).
[82] C. Du, H. Wang, F. Yang, and P. C. Hammel, Systematic variation of spin-orbit coupling with d-orbital filling: Large inverse spin hall effect in $3d$ transition metals, Phys. Rev. B **90**, 140407 (2014).
[83] M. Aoki, E. Shigematsu, R. Ohshima, T. Shinjo, M. Shiraishi, and Y. Ando, Anomalous sign inversion of spin-orbit torque in ferromagnetic/nonmagnetic bilayer systems due to self-induced spin-orbit torque, Phys. Rev. B **106**, 174418 (2022).
[84] R. E. Maizel, S. Wu, P. P. Balakrishnan, A. J. Grutter, C. J. Kinane, A. J. Caruana, P. Nakarmi, B. Nepal, D. A. Smith, Y. Lim, J. L. Jones, W. C. Thomas, J. Zhao, F. M. Michel, T. Mewes, and S. Emori, Vertically graded FeNi alloys with low damping and a sizeable spin-orbit torque, arXiv:2406.09874 (2024).
[85] M. W. Keller, K. S. Gerace, M. Arora, E. K. Delczeg-Czirjak, J. M. Shaw, and T. J. Silva, Near-unity spin hall ratio in Ni_xCu_{1-x} alloys, Phys. Rev. B **99**, 214411 (2019).
[86] D. Céspedes-Berrocal, H. Damas, S. Petit-Watelot, D. Maccariello, P. Tang, A. Arriola-Córdova, P. Vallobra, Y. Xu, J.-L. Bello, E. Martin, S. Migot, J. Ghanbaja, S. Zhang, M. Hehn, S. Mangin, C. Panagopoulos, V. Cros, A. Fert, and J.-C. Rojas-Sánchez, Current-induced spin torques on single gdfeco magnetic layers, Advanced Materials **33**, 2007047 (2021).
[87] M. B. Lifshits and M. I. Dyakonov, Swapping spin currents: Interchanging spin and flow directions, Phys. Rev. Lett. **103**, 186601 (2009).
[88] C. O. Pauyac, M. Chshiev, A. Manchon, and S. A. Nikolaev, Spin hall and spin swapping torques in diffusive ferromagnets, Phys. Rev. Lett. **120**, 176802 (2018).
[89] P. Gupta, I. J. Park, A. Swain, A. Mishra, V. P. Amin, and S. Bedanta, Self-induced inverse spin hall effect in $la_{0.67}sr_{0.33}mno_3$ films, Phys. Rev. B **109**, 014437 (2024).
[90] A. Vansteenkiste, J. Leliaert, M. Dvornik, M. Helsen, F. Garcia-Sanchez, and B. Van Waeyenberge, The design and verification of mumax3, AIP Advances **4**, 107133 (2014).
[91] L. D. Landau and E. M. Lifshitz, On the theory of the dispersion of magnetic permeability in ferromagnetic bodies (1935).
[92] T. L. Gilbert, A lagrangian formulation of the gyromagnetic equation of the magnetization field, Physical Review D **100**, 1243 (1955).
[93] G. Finocchio, I. N. Krivorotov, X. Cheng, L. Torres, and B. Azzerboni, Micromagnetic understanding of stochastic resonance driven by spin-transfer-torque, Phys. Rev. B **83**, 134402 (2011).
[94] J. Leliaert, J. Mulkers, J. De Clercq, A. Coene, M. Dvornik, and B. Van Waeyenberge, Adaptively time stepping the stochastic landau-lifshitz-gilbert equation at nonzero temperature: Implementation and validation in mumax3, AIP Advances **7**, 125010 (2017).
[95] W. F. Brown, Thermal fluctuations of a single-domain particle, Phys. Rev. **130**, 1677 (1963).
[96] H. Belrhazi, M. Y. El Hafidi, and M. El Hafidi, Micromagnetic simulation of current-induced magnetization dynamics in a half-heusler co1.5fe1.5ge alloy spin-valve nanopillar, SN Applied Sciences **1**, 41 (2018).
[97] P. Coelho, D. C. Leitao, J. Antunes, S. Cardoso, and P. P. Freitas, Spin valve devices with synthetic-ferrimagnet free-layer displaying enhanced sensitivity for nanometric sensors, IEEE Trans. Magn. **50**, 10.1109/TMAG.2014.2321044 (2014).
[98] E. A. Montoya, A. Khan, C. Safranski, A. Smith, and I. N. Krivorotov, Easy-plane spin hall oscillator, Commun. Phys. **6**, 184 (2023).
[99] S. Takei, Y. Tserkovnyak, and M. Mohseni, Spin superfluid josephson quantum devices, Phys. Rev. B **95**, 144402 (2017).
[100] M. A. W. Schoen, J. Lucassen, H. T. Nembach, B. Koopmans, T. J. Silva, C. H. Back, and J. M. Shaw, Magnetic properties in ultrathin 3d transition-metal binary alloys. ii. experimental verification of quantitative theories of damping and spin pumping, Phys. Rev. B **95**, 134411 (2017).
[101] D. A. Smith, A. Rai, Y. Lim, T. Hartnett, A. Sapkota, A. Srivastava, C. Mewes, Z. Jiang, M. Clavel, M. K. Hudait, D. D. Viehland, J. J. Heremans, P. V. Balachandran, T. Mewes, and S. Emori, Magnetic damping in epitaxial iron alloyed with vanadium and

aluminum, Phys. Rev. Appl. **14**, 034042 (2020).
[102] M. Arora, E. K. Delczeg-Czirjak, G. Riley, T. J. Silva, H. T. Nembach, O. Eriksson, and J. M. Shaw, Magnetic damping in polycrystalline thin-film Fe-V alloys, Phys. Rev. Applied **15**, 054031 (2021).
[103] S. S. P. Parkin, Origin of enhanced magnetoresistance of magnetic multilayers: Spin-dependent scattering from magnetic interface states, Phys. Rev. Lett. **71**, 1641 (1993).
[104] H. J. M. Swagten, G. J. Strijkers, P. J. H. Bloemen, M. M. H. Willekens, and W. J. M. de Jonge, Enhanced giant magnetoresistance in spin-valves sandwiched between insulating nio, Phys. Rev. B **53**, 9108 (1996).
[105] A. Hrabec, F. J. T. Gonçalves, C. S. Spencer, E. Arenholz, A. T. N'Diaye, R. L. Stamps, and C. H. Marrows, Spin-orbit interaction enhancement in permalloy thin films by pt doping, Phys. Rev. B **93**, 014432 (2016).
[106] S. Liang, L. Han, Y. You, H. Bai, F. Pan, and C. Song, Interface-relevant out-of-plane spin polarization in $Irmn_3$/permalloy bilayers, Phys. Rev. B **107**, 184427 (2023).
[107] A. Kumar, P. Gupta, N. Chowdhury, K. I. A. Khan, U. Shashank, S. Gupta, Y. Fukuma, S. Chaudhary, and P. K. Muduli, Interfacial origin of unconventional spin-orbit torque in py/irmn3, Advanced Quantum Technologies **6**, 2300092 (2023).
[108] K. Xia, P. J. Kelly, G. E. W. Bauer, A. Brataas, and I. Turek, Spin torques in ferromagnetic/normal-metal structures, Phys. Rev. B **65**, 220401 (2002).
[109] V. P. Amin, G. G. Baez Flores, A. A. Kovalev, and K. D. Belashchenko, Direct and indirect spin current generation and spin-orbit torques in ferromagnet/nonmagnet/ferromagnet trilayers, Phys. Rev. B **110**, 214427 (2024).
[110] R. Klause, Y. Xiao, J. Gibbons, V. P. Amin, K. D. Belashchenko, D. Go, E. E. Fullerton, and A. Hoffmann, Unconventional fieldlike spin torques in $crpt_3$, Phys. Rev. Appl. **22**, 044043 (2024).